

[Click here to view linked References](#)

1
2
3
4
5
6
7
8
9
10
11
12
13
14
15
16
17
18
19
20
21
22
23
24
25
26
27
28
29
30
31
32
33
34
35
36
37
38
39
40
41
42
43
44
45
46
47
48
49
50
51
52
53
54
55
56
57
58
59
60
61
62
63
64
65

Four Anti-Aging Drugs and Calorie-Restricted Diet Produce Parallel Effects in Fat, Brain, Muscle, Macrophages and Plasma of Young Mice

Xinna Li¹, Madaline McPherson², Mary Hager², Michael Lee², Peter Chang², Richard A. Miller^{1,3}

¹Department of Pathology, University of Michigan School of Medicine, Ann Arbor, Michigan 48109, USA

² College of Literature, Sciences, & the Arts, University of Michigan, Ann Arbor, Michigan 48109, USA

³ University of Michigan Geriatrics Center, Ann Arbor, Michigan 48109, USA

Corresponding author:

Xinna Li

email: xinna@umich.edu

office number: 734-936-2164

Mailing address: Room 3160, BSRB ,109 Zina Pitcher Place, Ann Arbor, MI 48109-2200.

ORCID: 0000-0002-7461-5628

1
2
3
4
5 **Abstract**
6

7 Average and maximal lifespan can be increased in mice, in one or both sexes, by four drugs:
8 rapamycin, acarbose, 17 α -estradiol, and canagliflozin. We show here that these four drugs, as
9 well as a calorie-restricted diet, can induce a common set of changes in fat, macrophages,
10 plasma, muscle, and brain when evaluated in young adults at 12 months of age. These shared
11 traits include an increase in uncoupling protein UCP1 in brown fat and in subcutaneous and
12 intra-abdominal white fat, a decline in proinflammatory M1 macrophages and corresponding
13 increase in anti-inflammatory M2 macrophages, an increase in muscle fibronectin type III
14 domain containing 5 (FNDC5) and its cleavage product irisin, and higher levels of doublecortin
15 (DCX) and brain-derived neurotrophic factor (BDNF) in brain. Each of these proteins is thought
16 to play a role in one or more age-related diseases, including metabolic, inflammatory, and
17 neurodegenerative diseases. We have previously shown that the same suite of changes is seen in
18 each of four varieties of slow-aging single-gene mutant mice. We propose that these changes
19 may be a part of a shared common pathway that is seen in slow-aging mice whether the delayed
20 aging is due to a mutation, a low-calorie diet, or a drug.
21
22

23
24 Key Words: uncoupling protein UCP1, inflammatory, neurodegenerative, slow-aging mice,
25 fibronectin type III domain containing 5 (FNDC5), doublecortin (DCX), and brain-derived
26 neurotrophic factor (BDNF).
27
28
29
30
31
32
33
34
35
36
37
38
39
40
41
42
43
44
45
46
47
48
49
50
51
52
53
54
55
56
57
58
59
60
61
62
63
64
65

Introduction

Several small compounds and dietary manipulations have been found to increase health-span and lifespan [1-3]. Canagliflozin (Cana) [4] and 17- α -estradiol (17 α E2) [5, 6] increase lifespan in males only, whereas calorie restriction (CR) [1], acarbose (Aca) [5], and rapamycin (Rapa) [7-9] increase lifespan in mice of both sexes, although the longevity effect of Aca is stronger in males than in females.

These agents affect health and aging through a variety of targets, not all of them fully delineated. Cana is a SGLT2 inhibitor used in the treatment of diabetes in humans [10, 11], Cana promotes release of urinary glucose under hyperglycemic conditions, and therefore decreases peak levels of glucose in the blood. Cana increased median lifespan of male mice by 14% with no change demonstrated in females [4]. Numerous studies have demonstrated the benefits of CR on the lifespan of organisms ranging from worms to humans, as well as its ability to delay or decelerate many aspects of aging [2, 3, 12, 13]. Rapa increases the lifespan of many organisms by inhibiting the mammalian target of rapamycin (mTOR) [14], Rapa can also diminish risks of cancer, cardiac diseases, neurodegenerative diseases, vascular aging, and cognitive function [15-19]. Like Cana, Aca reduces post-prandial glucose levels, and is used in the treatment of diabetics [20-22], but does so by inhibiting α -glucosidase conversion of starch to absorbable sugars in the GI tract. Like Rapa, Aca reduces mTOR signaling in liver and kidney [5, 23]. Mice treated with Aca showed a 20% increase in median lifespan in males and a smaller (5%) but statistically significant increase in females [5]. 17 α E2 is a non-feminizing structural isomer of 17- β estradiol [5, 6] that increases lifespan in male mice by 19%, without an effect on female lifespan [6]. Interestingly, Rapa and Aca lead to an increase in cap-independent translation (CIT) in both sexes, with a similar but male-specific increase induced by 17 α E2 [23]. The same pattern of drug effects is seen for inhibition of age-dependent increases in the kinase pathway, involving MEK1, Erk1/2, and MNK1/2, that regulates translation via phosphorylation of eIF4a [24]. These effects on protein translation suggest that these anti-aging drugs may share at least some common pathways and physiological mechanisms.

Aging decreases the size and activity of brown adipose tissue (BAT) depots, and lowers expression Uncoupling Protein 1 (UCP1), a mitochondrial membranous protein devoted to adaptive thermogenesis [25-27] via uncoupling of mitochondrial respiration [28-30]. UCP1-expressing adipocytes have also been found interspersed within white adipose tissue (WAT), in cells that exhibit a BAT-like phenotype, referred to as beige or “brite” (brown in white) fat [31]. Cold exposure and activation of β 3-adrenergic receptors by norepinephrine induce the expression of UCP1 in brown adipocytes and beige adipocytes [26, 32-35]. Mice with increased activity of brown fat, beige fat are resistant to obesity, and show improvements in systemic metabolism, including improved glucose tolerance and increased insulin sensitivity [36-39]. We have reported that white (WAT) and brown (BAT) fat have elevated UCP1 in four varieties of long-lived mutant mice, including Snell dwarf, Ames dwarf, and growth hormone receptor (GHR) knock-out mice, [40, 41], as well as in PAPP α -KO mice [42].

Aging typically leads to chronic, low-grade inflammation in adipose tissue [43-45], through activation of pro-inflammatory M1 macrophages polarization and conversion from M2 to M1 macrophages [46-48]. Adipose tissue macrophages (ATMs) play an important role in regulating inflammatory status within adipose tissue [49]. M1 macrophages typically express iNOS, while M2 cells are high in arginase. M1 macrophages secrete pro-inflammatory cytokines that inhibit insulin signaling within adipose tissue [50, 51]. M2 macrophages act opposite to their M1 counterpart. M2 macrophages are more anti-inflammatory and secrete anti-inflammatory cytokines that maintain functional insulin signaling [50, 51]. We have found that long-lived mutant mice, including Snell dwarf, Ames dwarf, growth hormone receptor (GHR) knock-out, and PAPP α -KO mice, showed lower levels of inflammatory M1 macrophages and higher levels of anti-inflammatory M2 macrophages in BAT and WAT, including both subcutaneous

1
2
3
4 (inguinal) and intra-abdominal (perigonadal) depots [40-42]. This suggests that skewing
5 macrophage polarization from pro-inflammatory M1 toward anti-inflammatory M2 phenotype
6 may contribute to the slow aging and delayed disease profile of these mutant mice.
7

8
9
10
11
12
13
14
15
16
17
18
19
20
21
22
23
24
25
26
27
28
29
30
31
32
33
34
35
36
37
38
39
40
41
42
43
44
45
46
47
48
49
50
51
52
53
54
55
56
57
58
59
60
61
62
63
64
65

Fibronectin type III domain-containing protein 5 (FNDC5) is primarily expressed by muscle fibers [52, 53]. FNDC5 is also expressed in heart, brain, ovary, testis, kidney, stomach, liver, and skeletal muscle tissues [54]. Under peroxisome proliferator-activated receptor gamma coactivator 1-alpha (PGC1 α) control, FNDC5 is cleaved and secreted as the hormone irisin in response to exercise. Irisin stimulates UCP1 expression and consequently induces browning in white adipose cells in culture and in vivo [39]. FNDC5/Irisin also has anti-inflammatory functions including reducing pro-inflammatory cytokines (IL-6, TNF- α , IL-1 β , and MIP), and increasing anti-inflammatory cytokines (IL-10, IL-4, and IL-1ra, and inducing M2-type macrophage polarization [55-57]. We have reported that irisin is elevated in the plasma of longevity mice (Snell, Ames, PAPP-A KO and GHRKO mice), consistent with a possible role in the modulation of adipose tissues, and further shown an increase of FNDC5 in muscle [40-42].

Brain Derived Neurotrophic Factor (BDNF) belongs to the neurotrophin family [58]. It is a key molecule in the regulation of neuronal plasticity related to learning and memory [59]. BDNF levels in hippocampus and plasma have been found to decrease with increasing age [59-61]. There is evidence that FNDC5 and irisin can stimulate brain derived neurotrophic factor (BDNF), which improves learning and memory through increased neuronal survival, differentiation, and plasticity [62, 63]. Doublecortin (DCX) is an essential factor in neurogenesis [64]. It is a nervous system-specific micro-tubule associated protein expressed in migrating neurons of the central and peripheral nervous system during embryonic and postnatal development [64-66]. The expression of DCX can be used in the adult brain as a measure of neural progenitor cells (NPCs), which generate new neurons in the dentate gyrus [67]. We have found elevation of both BDNF and DCX in the brain of all four of the long-lived mutant mouse stocks tested [68], but there is no current information about the possible effects of anti-aging drugs on these brain proteins.

GPLD1 (glycosylphosphatidylinositol-specific phospholipase D) is a plasma protein that is mainly liver-derived, but can also be produced by other tissues including brain, muscle, kidney, and immune cells [69]. GPLD1 production is increased through exercise in both mice and humans, and its function is to cleave GPI-anchored proteins from cell membranes. Increased levels of GPLD1 have been linked to an improvement in cognitive ability in aged mice [69]. We have reported [68] that GPLD1 protein is increased in liver and plasma of young adult Snell and GHRKO mice, Ames dwarf and PAPP-A-KO mice [41, 42]. Others have shown that augmented GPLD1 production in mice leads to increases in BDNF and DCX in brain [69], suggesting a connection between elevated GPLD1 in slow-aging mice and the accompanying increase in BDNF and DCX.

We have shown recently that drugs known to increase mouse lifespan can also lead to higher levels of GPLD1 in mouse liver and plasma [68]. Rapamycin and acarbose elevated GPLD1 in both sexes, but elevation of plasma GPLD1 by canagliflozin and 17 α E2 was seen only in male mice, consistent with the male-specific increase in lifespan induced by these two agents. A calorie restriction diet also elevated GPLD1 in both sexes. These results prompted us to ask whether other aspects of the phenotype seen in long-lived mutant mice, including changes in FNDC5, irisin, BDNF, DCX, UCP1, and M1/M2 macrophage ratios, might also be characteristic of mice exposed to drugs that extend lifespan and slow aging.

Materials and Methods

Mice and Experimental diets.

Genetically heterogeneous UM-HET3 mice were produced by a four-way cross between CByB6F1 mothers and C3D2F1 fathers and housed as previously described [9, 97]. Mice in breeding cages received Purina 5008 mouse chow, and weaned animals were fed Purina 5LG6. At 4 months of age, animals in different sibling groups were randomly allocated to control, Cana, CR, Aca, 17aE2, or Rapa treatments. All diets were prepared by TestDiet, Inc., a division of Purina Mills (Richmond, IN, USA), which also produces drug/food mixtures for the NIA Interventions Testing Program. Animals in the control group remained on the 5LG6 diet. Mice in the Cana group received this agent at 180 mg/kg of chow, i.e. 180 ppm [4]. Rapamycin was given as encapsulated Rapa (Emtora Biosciences, San Antonio, TX) at a dose of 14 ppm [7-9]. Aca was purchased from Spectrum Chemical Mfg. Corp. (Gardena, CA) and used at 1000 ppm [105]. 17aE2 was purchased from Steraloids Inc. (Newport, RI, USA) and used at a dose of 14.4 ppm [5, 105]. For CR feeding: starting at 4 months of age, CR mice were given 60% of diet consumed by ad lib control mice, as previously described [9]. All mice were then euthanized at 12 months of age.

Western blot analyses

Proteins from adipose tissues, thigh muscle, and brain cortex were extracted after homogenization in Immunoprecipitation Assay Buffer (RIPA Buffer, Fisher Scientific, Pittsburgh, PA, USA) supplemented with Complete Protease Inhibitor Cocktail (Roche Inc.). Protein content was measured using a BCA assay (Fisher Scientific, Pittsburgh, PA, USA). The protein extracts were separated by SDS/PAGE on a 4–15% running gel, transferred to polyvinylidene difluoride membranes, and electro-transferred to an Immobilon-P Transfer Membrane (Millipore, Billerica, MA, USA) for immune blot analyses. Membranes were blocked in Tris buffered saline containing 0.05% Tween20 (TBS-T) and 5% Bovine Serum Albumin (BSA) for 1 hour. After blocking, membranes were probed overnight with primary antibodies in TBS-T supplemented with 5% BSA with shaking at 4°C, followed by three 10-minute washes with TBS-T, incubation with secondary antibody for 1 hour, and three 10-minute washes with TBS-T. Membranes were then evaluated using an ECL Chemiluminescent Substrate (Fisher Scientific, Pittsburgh, PA, USA). Quantification was performed using ImageJ software. Table S1 lists the antibodies used.

Plasma irisin Measurement

Blood was collected from 12-month-old control mice and treated mice into EDTA-treated tubes. Plasma was separated from cells by centrifugation for 10 minutes at 1,000–2,000 x g using a refrigerated centrifuge. Plasma irisin concentration was determined by using a commercially available enzyme-linked immunosorbent assay (ELISA) kit (MyBioSource, Inc., USA) according to the manufacturer's instructions.

Statistical analysis

The data shown in each figure represent results of a minimum of three independent experiments. All data are presented as mean \pm SEM. Each endpoint was evaluated first by two-factor ANOVA, using Sex, Treatment, and Interaction terms. When the interaction test was not significant, the values were combined across sex and effects of treatment evaluated by unpaired two-tailed Student's t-test. When the interaction test was significant, data were separated by sex and effects of the treatment assessed by t-test separately for each sex independently. $P < 0.05$ was regarded as significant.

Results

UCP1 increases in BAT and WAT of five varieties of slow-aging mice. Our previous work has shown increased levels of UCP1 in BAT and in inguinal (ING) and perigonadal (PG) WAT fat depots of Snell dwarf, Ames dwarf, GHRKO, and PAPPa-KO mice [40-42]. To see if these changes could be produced by 8 months of exposure to an anti-aging diet (CR diet) or by anti-aging drugs, we evaluated fat tissues from 12 months old mice treated with the indicated interventions from 4 months of age. Figure 1 shows representative immunoblot images, with dotplots to show the distribution of densitometric results. For BAT, the two-way Anova found no evidence for sex specificity in the response to intervention (non-significant interaction term), and therefore results were pooled across sex for statistical assessment. Each of the five interventions increased UCP1 in BAT, with increases of 1.2 to 1.4, and p-values between 0.05 and 0.01 as shown in Fig 1B.

The effects of these interventions on UCP1 in both ING and PG WAT showed more evidence of sex-specificity. Cana, 17aE2, and CR diet each led to sex-specific effects, as indicated by the significant ANOVA interaction terms shown in Fig 1B. In each case the drug effect was larger in males than in females, both in ING and PG fat. Aca, in contrast, produced significant increases in UCP1 in both sexes, without any evidence of sex-specificity, again in both ING and PG fat. Rapa reduced UCP1 significantly without sex difference in both of these WAT depots.

Table 1 compiles the effect size (ratio of treated to control) and p-values for each sex evaluated separately for these UCP1 assays along with the other endpoints evaluated in this report.

Changes in fat-associated M1 and M2 macrophage subsets in slow-aging mice. Our studies of long-lived mutant mice showed increases in M2 macrophages and declines in the M1 macrophage subset in BAT and WAT [40]. Figure 2 shows drug- and diet-induced changes for Arg1, the M2 marker we used. Arg1 was elevated by CR and by all four drugs in BAT (Figure 2B). In ING WAT, Cana elevated Arg1 in males only ($p < 0.05$ for the ANOVA interaction term), and the other three drugs, along with CR, increased Arg1 in both sexes, although the 17aE2 effect may have been more potent in males ($p = 0.06$ for interaction). In PG WAT we saw Arg1 elevation in all five treatment groups, and there were no significant [sex x treatment] interactions.

Parallel data for the M1 marker iNOS are shown in Figure 3. As in the Snell and GHRKO mutants [40], each of the five tested interventions led to lower levels of iNOS in BAT, in PG WAT, and in ING WAT. For PG fat, there is suggestive evidence that the effect of 17aE2 might be stronger in males than in females ($p = 0.08$ for interaction). Decline in M1 cells is consistent with the evidence for an increase in M2 macrophages shown in Figure 2.

Muscle FNDC5 and plasma irisin changes were consistent with the effects on fat depots. Our work on GHRKO mice, and in mice where GHR was deleted only in muscle, found evidence that changes in fat and fat-associated macrophage subsets were dependent on elevated plasma irisin levels and to the levels of irisin-precursor FNDC5 in skeletal muscle [40]. We therefore looked at FNDC5 and plasma irisin in the five varieties of slow-aging mice in our current study. As shown in Figure 4B, muscle FNDC5 protein was significantly elevated by all five treatments. Plasma irisin, the secreted portion of the FNDC5 molecule, was also elevated significantly in all five kinds of treated mice (Figure 4C). For Cana and 17aE2 mice, the [sex x drug] interaction term approached statistical significance ($p = 0.07$ and 0.06 respectively), with slightly higher drug effects in the male mice. These data, along with the published results on Snell dwarf, GHRKO, and muscle-specific GHRKO [40], support the idea that the changes in the fat depots and fat-associated M1 and M2 subsets in diet- and drug-treated mice might be secondary to increases in muscle FNDC5 and plasma irisin.

1
2
3
4
5
6
7
8
9
10
11
12
13
14
15
16
17
18
19
20
21
22
23
24
25
26
27
28
29
30
31
32
33
34
35
36
37
38
39
40
41
42
43
44
45
46
47
48
49
50
51
52
53
54
55
56
57
58
59
60
61
62
63
64
65

Indices of neurogenesis and neural cell health in hippocampus of slow-aging mice. We have previously shown elevation of BDNF and DCX in hippocampus of Snell dwarf, GHRKO [68], Ames dwarf [41], and PAPPA-KO mice [42]. We therefore measured levels of both proteins in brain cortex of the five varieties of slow-aging mice, with results shown in Figure 5. All five interventions elevated both BDNF and DCX in brain. There were suggestions that the effects of Cana and 17aE2 might be relatively male-specific for BDNF, because $0.05 < p < 0.06$ for the ANOVA interaction terms for these two drugs.

In addition to effects of muscle - derived FNDC5 on adipose tissue, it has been reported recently [63, 70] that exercise can elevate FNDC5 in the mouse hippocampus, and thereby activate a neuroprotective program that includes elevation of BDNF. We therefore measured FNDC5 levels in brain of our five varieties of slow-aging mice (Figure 6). All five varieties of slow-aging mice had elevated levels of FNDC5 in brain cortex, with no evidence of significant sex-specificity.

Discussion

Our study shows that mice exposed to caloric restriction, or treated with drugs that extend lifespan, including rapamycin, acarbose, 17 α -estradiol, and canagliflozin, show increases in levels of UCP1 in WAT and BAT, increases in the ratio of M2 to M1 macrophages in fat depots, increases in the irisin precursor protein FNDC5 in skeletal muscle, increases in plasma irisin levels, and an increase in BDNF and DCX in the brain. These alterations are also characteristic of four varieties of slow-aging mutant mice: Ames dwarf, Snell dwarf, GKO, and Pappa-KO mice [40-42, 68]. Each of these proteins has been implicated as playing a role in maintenance of function in aging fat, brain, or metabolic and inflammatory control circuits, making it plausible that their elevation in mutant or drug-treated non-mutant mice might contribute to the exceptional preservation of good health in each of these nine models of slowed aging. The mechanism(s) through which the mutations, diet, or drugs induce these alterations in adipocytes, macrophages, muscle, and brain are not clear, but likely to be a fertile area for future study.

Uncoupling protein 1 (UCP1) is a mitochondrial membranous protein that contributes to adaptive thermogenesis in brown and beige adipocytes [27]. Cold acclimation or treatment with a β 3-adrenergic receptor agonist induces UCP1 expression in WAT, which mimics brown adipose tissue (WAT browning). These white adipose cells with similar BAT-like morphological features (such as smaller size, increased cytoplasm, and higher mitochondrial mass), and higher expression of UCP1, are referred to as "beige" fat cells [35, 71, 72]. Beige adipocytes have a high level of plasticity that allows for the rapid and dynamic induction of thermogenesis by external stimuli such as cold exposure [73]. Aging is characterized by an increase in WAT depot size, decreased amounts of BAT depots and in UCP1 levels within brown adipocytes, and a decline in the ability to induce fat browning in WAT depots [71]. Genetic and pharmacological interventions that increase characteristics of longevity in mice are often associated with resistance to age-related increases in intra-abdominal fat, with relative preservation of subcutaneous WAT depots [73]. The amount of BAT tissue, and level of UCP1 in BAT, are both increased in Ames dwarf mice [74], consistent with the idea that higher BAT thermogenic activity might contribute to longevity and health maintenance in Ames mice. For example, there is considerable evidence that UCP1-mediated uncoupling of the mitochondrial electron transport chain can augment beneficial health-related metabolic traits including beta oxidation of fatty acids and glucose homeostasis. In BAT, UCP1 is elevated by all four drugs and the CR diet, with Cana and 17 α E2 producing the change in males only. In both ING and PG WAT, sex-specificity was again seen for Cana and 17 α E2, and, unexpectedly, also for the CR diet, with greater effects in males in each case. The sex effect of these interventions (17 α E2 and Cana) on enhancing the function of BAT and induction in beige adipocyte formation is consistent with their effect on longevity. Aca led to changes in WAT in both sexes; this agent increases lifespan significantly in both sexes, though more dramatically in male mice. In contrast to the results of the other four treatments, Rapa led a lower UCP1 in both ING and PG WAT. We speculate that this may reflect direct or indirect effects of Rapa independent of those by which Rapa modulates the aging process.

Chronic low-grade inflammation is a common feature of age-related diseases and loss of homeostasis [75]. As a large and versatile endocrine, immune, and regenerative organ, adipose tissue plays both a direct and indirect role in chronic inflammation and consequently aging [76, 77]. Adipose tissue macrophages (ATM) have been considered to be key contributors to inflammation and insulin resistance [78, 79]. Macrophages have been classified as either classically (M1, proinflammatory), or alternatively (M2, anti-inflammatory) activated [80]. The M1 macrophage produces proinflammatory cytokines (e.g., IL-6 and TNF α), whereas the M2 macrophage secretes anti-inflammatory cytokines (e.g., IL-10). ATMs may also play a role in systemic or local adipose tissue inflammation. Aging typically leads to a change in polarization from anti-inflammatory M2 status to proinflammatory M1 macrophages in mice [80]. Using Arg1 protein levels as a marker for M2 cells and iNOS as a marker for M1 macrophages, our

1
2
3
4 previous study showed that M2 type macrophages were increased, with parallel decreases in M1
5 type macrophages, in BAT and two WAT depots of 6 months old Snell and GHRKO mice [40],
6 as well as in Ames and PAPP-A KO mice [41, 42]. Our work here showed elevation of Arg1 by
7 CR diet and by all four drugs in BAT and in both WAT depots. Cana had male-specific effects
8 on Arg1 in ING WAT and PG WAT, and the effects of 17aE2 on Arg1 in ING fat showed a
9 suggestive ($p = 0.06$) trend for male-specific effect. Using iNOS to identify M1 macrophages,
10 we found that each of the five tested interventions led to lower levels of iNOS in BAT, PG
11 WAT, and ING WAT. It is noteworthy that Aca and 17aE2 reduces age-dependent inflammatory
12 changes in the hypothalamus of male, but not female, mice [81], and Cana also blunts several
13 aspects of age-dependent inflammation in the hypothalamus, some in a sex-specific manner [82].
14 Whether the pathways by which these drugs modulate M1/M2 function in adipose tissue overlap
15 with those by which they diminish neuroinflammation is unknown and needs further study.
16
17

18 FNDC5 is a glycosylated type I membrane protein [52]. The cleaved and secreted form of
19 FNDC5 was discovered in 2012 and named “irisin”. The sequence of irisin is 100% conserved
20 between humans and mice [39]. Irisin has multiple effects, ranging from lipid metabolism,
21 thermogenesis, and browning of white adipose tissue, as well as ATM inflammation [83].
22 FNDC5 decreases adipose tissue inflammation and insulin resistance via AMPK-mediated
23 macrophage polarization in HFD-induced obesity [56]. FNDC5/irisin also induces the expression
24 of BDNF and other neuroprotective genes in the hippocampus [84]. Our previous work showed
25 enhanced levels of FNDC5 in muscle and increased levels of irisin in plasma of Snell dwarf
26 Ames dwarf, growth hormone receptor (GHR) knock-out mice, and PAPP-A-KO mice [40-42].
27 In our current study, FNDC5 protein in muscle was significantly elevated by CR and by all four
28 of the drugs tested, in both sexes. Irisin levels of plasma were consistent with the FNDC5 results:
29 each of the five interventions produced elevations of plasma irisin. There was a suggestion of
30 male-specific effect on irisin, with interaction p -values of 0.06 and 0.07 for 17aE2 and Cana,
31 respectively. These data, along with the published results on Snell dwarf, GHRKO, and muscle-
32 specific GHRKO [40], support the idea that the changes in the fat depots and fat-associated M1
33 and M2 subsets in diet and drug treated mice might be secondary to increases in muscle FNDC5
34 and plasma irisin. It seems likely that the changes in FNDC5 may underlie the alterations in
35 UCP1 and M1/M2 ratio in WAT of this series of mutant mice, but more work would be needed
36 to test this hypothesis.
37
38

39 Because we have previously shown that GPLD1 is elevated in liver and plasma of these CR and
40 drug-treated mice [68], evaluated BDNF and DCX in the brain; both of these indicators of brain
41 health are thought to be simulated by elevated GPLD1. Consistent with our earlier GPLD1
42 observations, BDNF and DCX were indeed higher in brain cortex of all five varieties of slow-
43 aging mice.
44

45 In addition to the effects FNDC5/irisin has on the WAT browning and macrophage polarization
46 [56, 83], it has been reported that exercise can elevate FNDC5 in the mouse hippocampus, and
47 thereby activate a neuroprotective program that includes elevation of BDNF [63, 70]. We
48 therefore measured FNDC5 levels in the brain of mice treated with anti-aging drugs or exposed
49 to the CR diet (Figure 6). All five varieties of slow-aging mice had elevated levels of FNDC5 in
50 the brain cortex. None of the drugs had a significant sex-specificity. These findings were
51 consistent with our previous data that showed an increase in FNDC5 in hippocampus of Ames,
52 Snell, and GHRKO mice [40, 41].
53
54

55 The research strategy for this paper emphasized breadth – evaluation of many tissues and cell
56 types in parallel – at the expense of a deeper analysis of any one of the cell types examined, and
57 this is a limitation of our study. To pick one example, we relied upon iNOS as our only index of
58 pro-inflammatory M1 macrophages, and on Arg1 as our estimator for anti-inflammatory M2
59 macrophages in the three fat depots studied. In an earlier paper focused on adipose tissue in
60 Snell dwarf and GHRKO mice [40], we used multiple methods for evaluation macrophage
61
62
63
64
65

1
2
3
4 polarity in fat depots, including (a) qRT-PCR data on mRNA for Arg1 and iNOS; (b)
5 immunohistochemical assessment of CD80 (a separate M1 marker) and CD163 (M2 marker) in
6 tissue sections, (c) measurement of CD80 and CD163 mRNA by qRT-PCR; and (d) RT-PCR
7 quantitation of three cytokines (TNF α , IL6, MCP1) produced by M1 cells. We performed this
8 entire test battery in three tissues: BAT, inguinal WAT, and perigonadal WAT. Consistency
9 among these tests was excellent, and all of them were consistent with the estimation of Arg1 and
10 iNOS levels by Western blots. It was also reassuring to see consistent reciprocity between the
11 M1 and M2 markers, which moved in opposite directions in both mutant mice, as in the data
12 presented here in our current paper. But it is an oversimplification to imagine that there are only
13 two differentiation states in the macrophage lineage without adipose tissue depots, and a more
14 careful and comprehensive study using additional methods would very probably lead to greater
15 nuance and additional insights into the status of macrophage polarization in these drug-treated
16 mice. Similarly, our data on BDNF and DCX in brain cortex are provocative, but leave
17 unanswered a wide range of questions related to other aspects of neural and glial status in young
18 adults, age-related changes in our drug-treated and CR mice, variation among CNS regions and
19 tissue layers, and other topics of very high interest. These limitations of our study provide, we
20 hope, ample opportunities for specialist laboratories to tease apart and exploit.

21
22
23 The work reported here, together with parallel studies of long-lived mutant mice [40, 41, 68],
24 suggest that slow-aging mice may share a suite of physiological characteristics, regardless of
25 whether the extended longevity is caused by an inherited mutation, or by treatment with a drug
26 or dietary regime starting in adult life. This suite of “aging rate indicators” seems to include
27 increases in UCP1, M2/M1 ratio at least in adipose tissue, FNCD5/irisin in muscle, GPLD1
28 production by liver and adipose tissue, and increases in BDNF and DCX in brain. Mutant and
29 drug-treated slow-aging mice are also characterized by augmented cap-independent translation
30 [23, 85], by lower function of mTORC1 [86], and by inhibition of two distinct MAP kinase
31 cascades [24]. It seems likely that future work may add additional shared characteristics to this
32 set of changes. Working out the cellular basis for this apparently coordinated set of changes is an
33 important challenge for future studies, along with exploration of links between these changes and
34 the delayed pace of multiple lethal and non-lethal diseases in these mice. It is also possible that
35 some or all of these alterations can serve as surrogate endpoints that can identify drugs with good
36 potential to delay aging.

37 38 39 40 **Acknowledgements:**

41
42 We thank Lori Roberts, Natalie Perry, Roxann Alonzo, Jacob Sheets and Ilkim Erturk for expert
43 assistance in animal care. The work was supported by a grant from the Glenn Foundation for
44 Medical Research, and by NIH grants AG023122 and AG024824.

45 46 **Conflict of interest:**

47
48 The authors have stated explicitly that there are no conflicts of interest in connection with this
49 article.

50 51 52 **Author contributions:**

53
54 X.L. designed and did the experiments and wrote the manuscript. M.M., M.L., M.H., and P.C.
55 helped with experiments. P.C. did western blotting experiments. R.A.M. helped design the
56 experiments and to edit the manuscript.

57 58 **Data availability:**

59
60
61
62
63
64
65

1
2
3
4
5
6
7
8
9
10
11
12
13
14
15
16
17
18
19
20
21
22
23
24
25
26
27
28
29
30
31
32
33
34
35
36
37
38
39
40
41
42
43
44
45
46
47
48
49
50
51
52
53
54
55
56
57
58
59
60
61
62
63
64
65

All raw images, densitometric data, and statistical calculations are available from the authors (XL, RAM) on request.

1
2
3
4 **Legends to Figures:**
5

6 **Figure 1: Expression of UCP1 in adipose tissue of five varieties of slow-aging mice.**
7

8
9 **A.** Cell lysates were prepared from adipose tissues (brown adipose tissue, inguinal adipose tissue and perigonadal adipose tissue) of 48-week-old wild type littermate control mice (WT) and mice treated with the indicated interventions (CR diet, Cana, 17aE2, Aca and Rapa) from 4 months of age. Protein levels of UCP1 (brown and beige fat marker) were measured by western blotting. Representative gel images showing UCP1 in brown adipose tissue, inguinal adipose tissue and perigonadal adipose tissue. **B.** Protein quantification data normalized to β -actin and expressed as fold change compared with WT control (defined as 1.0). For BAT and PG WAT, N = 5 mice for each group (control and slow-aging mice). For ING WAT, N = 8 mice for each group (control and slow-aging mice). Each symbol shows an individual mouse. * $p < 0.05$; ** $p < 0.01$, *** $p < 0.001$ versus control mice.
10
11
12
13
14
15
16
17
18
19

20 **Figure 2: Expression of adipose tissue macrophage infiltration and M2 macrophage marker in adipose tissue of five varieties of slow-aging mice.**
21
22

23
24 **A.** Cell lysates were prepared from adipose tissues (brown adipose tissue, inguinal adipose tissue and perigonadal adipose tissue) of 48-week-old wild type littermate control mice (WT) and mice treated with the indicated interventions (CR diet, Cana, 17aE2, Aca and Rapa) from 4 months of age. Protein levels of Arg1 (M2 macrophage marker) were measured by western blotting. Representative gel images showing Arg1 in brown adipose tissue, inguinal adipose tissue and perigonadal adipose tissue. **B.** Protein quantification data normalized to β -actin and expressed as fold change compared with WT control (defined as 1.0 For BAT and PG WAT, N = 5 mice for each group (control and slow-aging mice). For ING WAT, N = 8 mice for each group (control and slow-aging mice). Each symbol shows an individual mouse. * $p < 0.05$; ** $p < 0.01$, *** $p < 0.001$ versus control mice.
25
26
27
28
29
30
31
32
33
34

35 **Figure 3: Expression of adipose tissue macrophage infiltration and M1 macrophage marker in adipose tissue of five varieties of slow-aging mice.**
36
37

38
39 **A.** Cell lysates were prepared from adipose tissues (brown adipose tissue, inguinal adipose tissue and perigonadal adipose tissue) of 48-week-old wild type littermate control mice (WT) and mice treated with the indicated interventions (CR diet, Cana, 17aE2, Aca and Rapa) from 4 months of age. Protein levels of iNOS (M1 macrophage marker) were measured by western blotting. Representative gel images showing iNOS in brown adipose tissue, inguinal adipose tissue and perigonadal adipose tissue. **B.** Protein quantification data normalized to β -actin and expressed as fold change compared with WT control (defined as 1.0 For BAT and PG FAT, N = 5 mice for each group (WT and slow-aging mice). For ING FAT, N = 8 mice for each group (WT and slow-aging mice). Each symbol shows an individual mouse. * $p < 0.05$; ** $p < 0.01$, *** $p < 0.001$ versus control mice.
40
41
42
43
44
45
46
47
48
49

50 **Figure 4: Expression of FNDC5 in thigh muscle and plasma irisin levels of five varieties of slow-aging mice.**
51
52

53
54 **A.** Cell lysates were prepared from thigh muscle of 48-week-old wild type littermate control mice (WT) and mice treated with the indicated interventions (CR diet, Cana, 17aE2, Aca and Rapa) from 4 months of age. Protein levels of FNDC5 were measured by western blotting. Representative gel images are shown. **B.** Protein quantification data normalized to β -actin and expressed as fold change compared with WT control (defined as 1.0). N = 5 mice for each group (WT and slow-aging mice). Data are means \pm SEM. * $P < 0.05$, ** $P < 0.01$, *** $P < 0.001$ versus WT. **C.** Irisin content was measured by ELISA assay on plasma samples of 48-week-old
55
56
57
58
59
60
61
62
63
64
65

1
2
3
4 wild type littermate control mice (WT) and five varieties of slow-aging mice (Cana, CR, ACA,
5 17aE2 and Rapa). N = 6 per group. Each symbol shows an individual mouse. * p < 0.05; ** p <
6 0.01, *** p < 0.001 versus control mice.
7

8 **Figure 5: Expression of BDNF and doublecortin (Dcx) in brain cortex of five varieties of**
9 **slow-aging mice.**

10
11 **A.** Cell lysates were prepared from brain cortex of 48-week-old wild type littermate control mice
12 (WT) and mice treated with the indicated interventions (CR diet, Cana, 17aE2, Aca and Rapa)
13 from 4 months of age. Protein levels of BDNF and Dcx were measured by western blotting.
14 Representative gel images are shown. **B.** Protein quantification data normalized to β -actin and
15 expressed as fold change compared with WT control (defined as 1.0). N = 5 mice for each group
16 (WT and slow-aging mice. Each symbol shows an individual mouse. * p < 0.05; ** p < 0.01, ***
17 p < 0.001 versus control mice.
18
19
20

21 **Figure 6: Expression of FNDC5 in brain cortex of five varieties of slow-aging mice.**

22
23 **A.** Cell lysates were prepared from brain cortex of 48-week-old wild type littermate control mice
24 (WT) and mice treated with the indicated interventions (CR diet, Cana, 17aE2, Aca and Rapa)
25 from 4 months of age. Protein levels of FNDC5 were measured by western blotting.
26 Representative gel images are shown. **B.** Protein quantification data normalized to β -actin and
27 expressed as fold change compared with WT control (defined as 1.0). N = 5 mice for each group
28 (WT and slow-aging mice. Each symbol shows an individual mouse. * p < 0.05; ** p < 0.01, ***
29 p < 0.001 versus control mice.
30
31
32
33
34
35
36
37
38
39
40
41
42
43
44
45
46
47
48
49
50
51
52
53
54
55
56
57
58
59
60
61
62
63
64
65

References cited

1. Fontana, L., L. Partridge, and V.D. Longo, *Extending healthy life span--from yeast to humans*. Science, 2010. **328**(5976): p. 321-6.
2. Ravussin, E., et al., *A 2-Year Randomized Controlled Trial of Human Caloric Restriction: Feasibility and Effects on Predictors of Health Span and Longevity*. J Gerontol A Biol Sci Med Sci, 2015. **70**(9): p. 1097-104.
3. Mattison, J.A., et al., *Caloric restriction improves health and survival of rhesus monkeys*. Nat Commun, 2017. **8**: p. 14063.
4. Miller, R.A., et al., *Canagliflozin extends life span in genetically heterogeneous male but not female mice*. JCI Insight, 2020. **5**(21).
5. Harrison, D.E., et al., *Acarbose, 17- α -estradiol, and nordihydroguaiaretic acid extend mouse lifespan preferentially in males*. Aging Cell, 2014. **13**(2): p. 273-82.
6. Strong, R., et al., *Longer lifespan in male mice treated with a weakly estrogenic agonist, an antioxidant, an α -glucosidase inhibitor or a Nrf2-inducer*. Aging Cell, 2016. **15**(5): p. 872-84.
7. Harrison, D.E., et al., *Rapamycin fed late in life extends lifespan in genetically heterogeneous mice*. Nature, 2009. **460**(7253): p. 392-5.
8. Miller, R.A., et al., *Rapamycin, but not resveratrol or simvastatin, extends life span of genetically heterogeneous mice*. J Gerontol A Biol Sci Med Sci, 2011. **66**(2): p. 191-201.
9. Miller, R.A., et al., *Rapamycin-mediated lifespan increase in mice is dose and sex dependent and metabolically distinct from dietary restriction*. Aging Cell, 2014. **13**(3): p. 468-77.
10. Ohgaki, R., et al., *Interaction of the Sodium/Glucose Cotransporter (SGLT) 2 inhibitor Canagliflozin with SGLT1 and SGLT2*. J Pharmacol Exp Ther, 2016. **358**(1): p. 94-102.
11. Nomura, S., et al., *Discovery of canagliflozin, a novel C-glucoside with thiophene ring, as sodium-dependent glucose cotransporter 2 inhibitor for the treatment of type 2 diabetes mellitus*. J Med Chem, 2010. **53**(17): p. 6355-60.
12. Kapahi, P., M. Kaeberlein, and M. Hansen, *Dietary restriction and lifespan: Lessons from invertebrate models*. Ageing Res Rev, 2017. **39**: p. 3-14.
13. Flanagan, E.W., et al., *Calorie Restriction and Aging in Humans*. Annu Rev Nutr, 2020. **40**: p. 105-133.
14. Johnson, S.C., P.S. Rabinovitch, and M. Kaeberlein, *mTOR is a key modulator of ageing and age-related disease*. Nature, 2013. **493**(7432): p. 338-45.
15. Lashinger, L.M., et al., *Rapamycin partially mimics the anticancer effects of calorie restriction in a murine model of pancreatic cancer*. Cancer Prev Res (Phila), 2011. **4**(7): p. 1041-51.
16. Hussein, O., et al., *Rapamycin inhibits osteolysis and improves survival in a model of experimental bone metastases*. Cancer Lett, 2012. **314**(2): p. 176-84.
17. Zhao, L., et al., *Low-dose oral sirolimus reduces atherogenesis, vascular inflammation and modulates plaque composition in mice lacking the LDL receptor*. Br J Pharmacol, 2009. **156**(5): p. 774-85.
18. Jahrling, J.B., et al., *mTOR drives cerebral blood flow and memory deficits in LDLR(-/-) mice modeling atherosclerosis and vascular cognitive impairment*. J Cereb Blood Flow Metab, 2018. **38**(1): p. 58-74.
19. Tramutola, A., et al., *Intranasal rapamycin ameliorates Alzheimer-like cognitive decline in a mouse model of Down syndrome*. Transl Neurodegener, 2018. **7**: p. 28.
20. Madar, Z. and A. Hazan, *Effect of miglitol and acarbose on starch digestion, daily plasma glucose profiles and cataract formation*. J Basic Clin Physiol Pharmacol, 1993. **4**(1-2): p. 69-81.
21. Madar, Z., A. Hazan, and A. Pollack, *Beneficial effects of acarbose on daily plasma glucose profile and cataract development in sand rats*. Eye (Lond), 1994. **8** (Pt 3): p. 353-6.

- 1
 - 2
 - 3
 - 4
 - 5
 - 6
 - 7
 - 8
 - 9
 - 10
 - 11
 - 12
 - 13
 - 14
 - 15
 - 16
 - 17
 - 18
 - 19
 - 20
 - 21
 - 22
 - 23
 - 24
 - 25
 - 26
 - 27
 - 28
 - 29
 - 30
 - 31
 - 32
 - 33
 - 34
 - 35
 - 36
 - 37
 - 38
 - 39
 - 40
 - 41
 - 42
 - 43
 - 44
 - 45
 - 46
 - 47
 - 48
 - 49
 - 50
 - 51
 - 52
 - 53
 - 54
 - 55
 - 56
 - 57
 - 58
 - 59
 - 60
 - 61
 - 62
 - 63
 - 64
 - 65
22. Wolf, T., et al., *The MalR type regulator AcrC is a transcriptional repressor of acarbose biosynthetic genes in Actinoplanes sp. SE50/110*. BMC Genomics, 2017. **18**(1): p. 562.
23. Shen, Z., et al., *Cap-independent translation: A shared mechanism for lifespan extension by rapamycin, acarbose, and 17 α -estradiol*. Aging Cell, 2021. **20**(5): p. e13345.
24. Wink, L., R.A. Miller, and G.G. Garcia, *Rapamycin, Acarbose and 17 α -estradiol share common mechanisms regulating the MAPK pathways involved in intracellular signaling and inflammation*. Immun Ageing, 2022. **19**(1): p. 8.
25. Graja, A. and T.J. Schulz, *Mechanisms of aging-related impairment of brown adipocyte development and function*. Gerontology, 2015. **61**(3): p. 211-7.
26. Rogers, N.H., et al., *Aging leads to a programmed loss of brown adipocytes in murine subcutaneous white adipose tissue*. Aging Cell, 2012. **11**(6): p. 1074-83.
27. Ricquier, D., *Uncoupling protein 1 of brown adipocytes, the only uncoupler: a historical perspective*. Front Endocrinol (Lausanne), 2011. **2**: p. 85.
28. Thomas, S.A. and R.D. Palmiter, *Thermoregulatory and metabolic phenotypes of mice lacking noradrenaline and adrenaline*. Nature, 1997. **387**(6628): p. 94-7.
29. Aquila, H., T.A. Link, and M. Klingenberg, *The uncoupling protein from brown fat mitochondria is related to the mitochondrial ADP/ATP carrier. Analysis of sequence homologies and of folding of the protein in the membrane*. Embo j, 1985. **4**(9): p. 2369-76.
30. Heaton, G.M., et al., *Brown-adipose-tissue mitochondria: photoaffinity labelling of the regulatory site of energy dissipation*. Eur J Biochem, 1978. **82**(2): p. 515-21.
31. Vitali, A., et al., *The adipose organ of obesity-prone C57BL/6J mice is composed of mixed white and brown adipocytes*. J Lipid Res, 2012. **53**(4): p. 619-29.
32. Petrovic, N., et al., *Chronic peroxisome proliferator-activated receptor gamma (PPAR γ) activation of epididymally derived white adipocyte cultures reveals a population of thermogenically competent, UCP1-containing adipocytes molecularly distinct from classic brown adipocytes*. J Biol Chem, 2010. **285**(10): p. 7153-64.
33. Ishibashi, J. and P. Seale, *Medicine. Beige can be slimming*. Science, 2010. **328**(5982): p. 1113-4.
34. Rosen, E.D. and B.M. Spiegelman, *What we talk about when we talk about fat*. Cell, 2014. **156**(1-2): p. 20-44.
35. Cannon, B. and J. Nedergaard, *Brown adipose tissue: function and physiological significance*. Physiol Rev, 2004. **84**(1): p. 277-359.
36. Bordicchia, M., et al., *Cardiac natriuretic peptides act via p38 MAPK to induce the brown fat thermogenic program in mouse and human adipocytes*. J Clin Invest, 2012. **122**(3): p. 1022-36.
37. Cederberg, A., et al., *FOXC2 is a winged helix gene that counteracts obesity, hypertriglyceridemia, and diet-induced insulin resistance*. Cell, 2001. **106**(5): p. 563-73.
38. Seale, P., et al., *Prdm16 determines the thermogenic program of subcutaneous white adipose tissue in mice*. J Clin Invest, 2011. **121**(1): p. 96-105.
39. Boström, P., et al., *A PGC1- α -dependent myokine that drives brown-fat-like development of white fat and thermogenesis*. Nature, 2012. **481**(7382): p. 463-8.
40. Li, X., et al., *Muscle-dependent regulation of adipose tissue function in long-lived growth hormone-mutant mice*. Aging (Albany NY), 2020. **12**(10): p. 8766-8789.
41. Li, X., et al., *Transient early life growth hormone exposure permanently alters brain, muscle, liver, macrophage, and adipocyte status in long-lived Ames dwarf mice*. Faseb j, 2022. **36**(7): p. e22394.
42. Li, X., et al., *Recapitulation of anti-aging phenotypes by global, but not by muscle-specific, deletion of PAPP-A in mice*. Geroscience, 2022.
43. Kraakman, M.J., et al., *Macrophage polarization in obesity and type 2 diabetes: weighing down our understanding of macrophage function?* Front Immunol, 2014. **5**: p. 470.
44. Patsouris, D., et al., *Insulin resistance is associated with MCP1-mediated macrophage accumulation in skeletal muscle in mice and humans*. PLoS One, 2014. **9**(10): p. e110653.

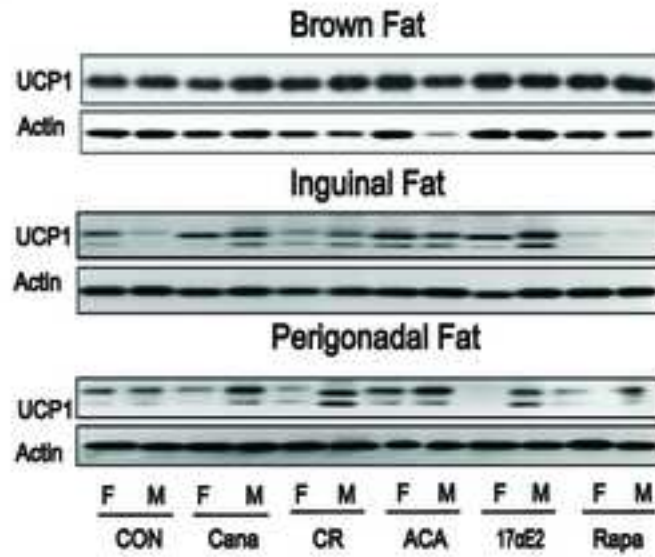
- 1
- 2
- 3
- 4 45. Fuentes, L., T. Roszer, and M. Ricote, *Inflammatory mediators and insulin resistance in obesity: role of nuclear receptor signaling in macrophages*. *Mediators Inflamm*, 2010. **2010**: p. 219583.
- 7 46. Costantini, A., et al., *Age-related M1/M2 phenotype changes in circulating monocytes from healthy/unhealthy individuals*. *Aging (Albany NY)*, 2018. **10(6)**: p. 1268-1280.
- 9 47. Mahbub, S., C.R. Deburghraeve, and E.J. Kovacs, *Advanced age impairs macrophage polarization*. *J Interferon Cytokine Res*, 2012. **32(1)**: p. 18-26.
- 12 48. Mills, C.D., et al., *M-1/M-2 macrophages and the Th1/Th2 paradigm*. *J Immunol*, 2000. **164(12)**: p. 6166-73.
- 14 49. Morris, D.L., K. Singer, and C.N. Lumeng, *Adipose tissue macrophages: phenotypic plasticity and diversity in lean and obese states*. *Curr Opin Clin Nutr Metab Care*, 2011. **14(4)**: p. 341-6.
- 17 50. Russo, L. and C.N. Lumeng, *Properties and functions of adipose tissue macrophages in obesity*. *Immunology*, 2018. **155(4)**: p. 407-417.
- 19 51. Thomas, D. and C. Apovian, *Macrophage functions in lean and obese adipose tissue*. *Metabolism*, 2017. **72**: p. 120-143.
- 21 52. Ferrer-Martínez, A., P. Ruiz-Lozano, and K.R. Chien, *Mouse PeP: a novel peroxisomal protein linked to myoblast differentiation and development*. *Dev Dyn*, 2002. **224(2)**: p. 154-67.
- 24 53. Teufel, A., et al., *Frcp1 and Frcp2, two novel fibronectin type III repeat containing genes*. *Gene*, 2002. **297(1-2)**: p. 79-83.
- 26 54. Huh, J.Y., et al., *FNDC5 and irisin in humans: I. Predictors of circulating concentrations in serum and plasma and II. mRNA expression and circulating concentrations in response to weight loss and exercise*. *Metabolism*, 2012. **61(12)**: p. 1725-38.
- 29 55. Mazur-Bialy, A.I., E. Pochech, and M. Zarawski, *Anti-Inflammatory Properties of Irisin, Mediator of Physical Activity, Are Connected with TLR4/MyD88 Signaling Pathway Activation*. *Int J Mol Sci*, 2017. **18(4)**.
- 32 56. Xiong, X.Q., et al., *FNDC5 attenuates adipose tissue inflammation and insulin resistance via AMPK-mediated macrophage polarization in obesity*. *Metabolism*, 2018. **83**: p. 31-41.
- 36 57. Matsuo, Y., et al., *Fibronectin type III domain containing 5 expression in skeletal muscle in chronic heart failure-relevance of inflammatory cytokines*. *J Cachexia Sarcopenia Muscle*, 2015. **6(1)**: p. 62-72.
- 39 58. Huang, E.J. and L.F. Reichardt, *Neurotrophins: roles in neuronal development and function*. *Annu Rev Neurosci*, 2001. **24**: p. 677-736.
- 41 59. MacPherson, R.E.K., *Filling the void: a role for exercise-induced BDNF and brain amyloid precursor protein processing*. *Am J Physiol Regul Integr Comp Physiol*, 2017. **313(5)**: p. R585-r593.
- 44 60. Bednarski, E., et al., *Lysosomal dysfunction reduces brain-derived neurotrophic factor expression*. *Exp Neurol*, 1998. **150(1)**: p. 128-35.
- 46 61. Karege, F., M. Schwald, and M. Cisse, *Postnatal developmental profile of brain-derived neurotrophic factor in rat brain and platelets*. *Neurosci Lett*, 2002. **328(3)**: p. 261-4.
- 48 62. Pignataro, P., et al., *FNDC5/Irisin System in Neuroinflammation and Neurodegenerative Diseases: Update and Novel Perspective*. *Int J Mol Sci*, 2021. **22(4)**.
- 50 63. Wrann, C.D., et al., *Exercise induces hippocampal BDNF through a PGC-1 α /FNDC5 pathway*. *Cell Metab*, 2013. **18(5)**: p. 649-59.
- 52 64. Gleeson, J.G., et al., *Doublecortin is a microtubule-associated protein and is expressed widely by migrating neurons*. *Neuron*, 1999. **23(2)**: p. 257-71.
- 54 65. Francis, F., et al., *Doublecortin is a developmentally regulated, microtubule-associated protein expressed in migrating and differentiating neurons*. *Neuron*, 1999. **23(2)**: p. 247-56.
- 57 66. Couillard-Despres, S., et al., *Doublecortin expression levels in adult brain reflect neurogenesis*. *Eur J Neurosci*, 2005. **21(1)**: p. 1-14.
- 60
- 61
- 62
- 63
- 64
- 65

- 1
2
3
4 67. Balthazart, J. and G.F. Ball, *Doublecortin is a highly valuable endogenous marker of adult neurogenesis in canaries. Commentary on Vellema M et al. (2014): Evaluating the predictive value of doublecortin as a marker for adult neurogenesis in canaries (Serinus canaria)*. *J Comparative Neurol* 522:1299-1315. *Brain Behav Evol*, 2014. **84**(1): p. 1-4.
- 5
6
7
8 68. Li, X., et al., *Cap-independent translation of GPLD1 enhances markers of brain health in long-lived mutant and drug-treated mice*. *Aging Cell*, 2022: p. e13685.
- 9
10 69. Horowitz, A.M., et al., *Blood factors transfer beneficial effects of exercise on neurogenesis and cognition to the aged brain*. *Science*, 2020. **369**(6500): p. 167-173.
- 11
12 70. Wrann, C.D., *FNDC5/irisin - their role in the nervous system and as a mediator for beneficial effects of exercise on the brain*. *Brain Plast*, 2015. **1**(1): p. 55-61.
- 13
14 71. Young, P., J.R. Arch, and M. Ashwell, *Brown adipose tissue in the parametrial fat pad of the mouse*. *FEBS Lett*, 1984. **167**(1): p. 10-4.
- 15
16 72. Cousin, B., et al., *Occurrence of brown adipocytes in rat white adipose tissue: molecular and morphological characterization*. *J Cell Sci*, 1992. **103 (Pt 4)**: p. 931-42.
- 17
18 73. Stout, M.B., et al., *Growth hormone action predicts age-related white adipose tissue dysfunction and senescent cell burden in mice*. *Aging (Albany NY)*, 2014. **6**(7): p. 575-86.
- 19
20 74. Darcy, J., et al., *Brown Adipose Tissue Function Is Enhanced in Long-Lived, Male Ames Dwarf Mice*. *Endocrinology*, 2016. **157**(12): p. 4744-4753.
- 21
22 75. Salminen, A., *Increased immunosuppression impairs tissue homeostasis with aging and age-related diseases*. *J Mol Med (Berl)*, 2021. **99**(1): p. 1-20.
- 23
24 76. Scheja, L. and J. Heeren, *The endocrine function of adipose tissues in health and cardiometabolic disease*. *Nat Rev Endocrinol*, 2019. **15**(9): p. 507-524.
- 25
26 77. van der Heijden, R.A., et al., *High-fat diet induced obesity primes inflammation in adipose tissue prior to liver in C57BL/6j mice*. *Aging (Albany NY)*, 2015. **7**(4): p. 256-68.
- 27
28 78. Weisberg, S.P., et al., *Obesity is associated with macrophage accumulation in adipose tissue*. *J Clin Invest*, 2003. **112**(12): p. 1796-808.
- 29
30 79. Xu, H., et al., *Chronic inflammation in fat plays a crucial role in the development of obesity-related insulin resistance*. *J Clin Invest*, 2003. **112**(12): p. 1821-30.
- 31
32 80. Lumeng, C.N., J.L. Bodzin, and A.R. Saltiel, *Obesity induces a phenotypic switch in adipose tissue macrophage polarization*. *J Clin Invest*, 2007. **117**(1): p. 175-84.
- 33
34 81. Sadagurski, M., G. Cady, and R.A. Miller, *Anti-aging drugs reduce hypothalamic inflammation in a sex-specific manner*. *Aging Cell*, 2017. **16**(4): p. 652-660.
- 35
36 82. Jayarathne, H.S.M., et al., *Neuroprotective effects of Canagliflozin: Lessons from aged genetically diverse UM-HET3 mice*. *Aging Cell*, 2022. **21**(7): p. e13653.
- 37
38 83. Zhang, Y., et al., *Irisin exerts dual effects on browning and adipogenesis of human white adipocytes*. *Am J Physiol Endocrinol Metab*, 2016. **311**(2): p. E530-41.
- 39
40 84. Liu, P., et al., *Quercetin ameliorates hypobaric hypoxia-induced memory impairment through mitochondrial and neuron function adaptation via the PGC-1 α pathway*. *Restor Neurol Neurosci*, 2015. **33**(2): p. 143-57.
- 41
42 85. Ozkurede, U., et al., *Cap-independent mRNA translation is upregulated in long-lived endocrine mutant mice*. *J Mol Endocrinol*, 2019. **63**(2): p. 123-138.
- 43
44 86. Dominick, G., et al., *Regulation of mTOR activity in Snell dwarf and GH receptor gene-disrupted mice*. *Endocrinology*, 2015. **156**(2): p. 565-75.
- 45
46
47
48
49
50
51
52
53
54
55
56
57
58
59
60
61
62
63
64
65

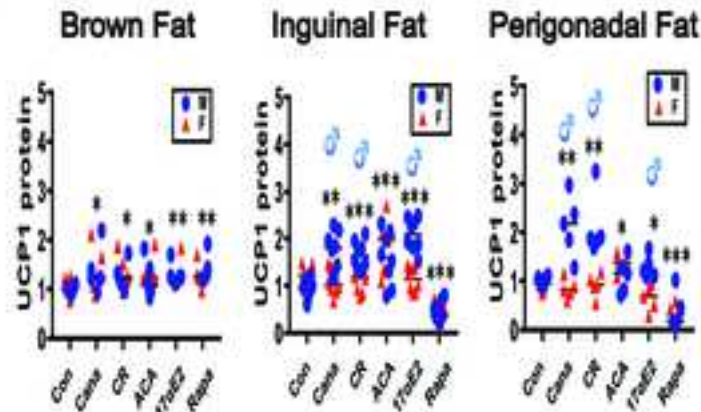
Table 1: Collection of statistical results

Protein	Tissue	Cana	CR	Aca	17aE2	Rapa
UCP1	BAT	M: 1.4x, p < 0.05 F: 1.4x, p < 0.05	M: 1.3x, p < 0.05 F: 1.4x, p < 0.05	M: 1.2x, p < 0.05 F: 1.4x, p < 0.05	M: 1.3x, p < 0.05 F: 1.4x, p < 0.01	M: 1.4x, p < 0.05 F: 1.3x, p < 0.05
UCP1	ING WAT	M: 1.7x, p < 0.001 F: 1.1x, p =0.67	M: 1.7x, p < 0.001 F: 1.1x, p =0.72	M: 1.6x, p < 0.001 F: 1.8x, p < 0.01	M: 2.1x, p < 0.001 F: 1.1x, p =0.78	M: 0.4x, p < 0.001 F: 0.4x, p < 0.001
UCP1	PG WAT	M: 2.2x, p < 0.01 F: 0.9x, p =0.46	M: 1.9x, p < 0.01 F: 1.0x, p =0.89	M: 1.3x, p < 0.05 F: 1.3x, p < 0.05	M: 1.3x, p < 0.01 F: 0.7x, p =0.07	M: 0.4x, p < 0.01 F: 0.3x, p <0.05
Arg1	BAT	M: 1.8x, p < 0.01 F: 1.6x, p < 0.01	M: 1.5x, p < 0.05 F: 1.5x, p < 0.05	M: 1.7x, p < 0.01 F: 1.9x, p < 0.05	M: 1.6x, p < 0.05 F: 1.7x, p < 0.01	M: 1.6x, p < 0.05 F: 1.8x, p < 0.01
Arg1	ING WAT	M: 1.6x, p < 0.01 F: 1x, p = 0.78	M: 1.5x, p < 0.05 F: 1.4x, p < 0.05	M: 1.6x, p < 0.05 F: 1.5x, p < 0.05	M: 1.4x, p < 0.01 F: 1.1x, p = 0.89	M: 1.5x, p < 0.05 F: 1.4x, p <0.05
Arg1	PG WAT	M: 1.6x, p < 0.05 F: 1.0x, p =0.54	M: 1.8x, p < 0.01 F: 1.5x, p < 0.05	M: 1.7x, p < 0.05 F: 1.7x, p < 0.01	M: 1.9x, p < 0.01 F: 1.3x, p =0.21	M: 1.2x, p < 0.05 F: 1.3x, p <0.05
iNOS	BAT	M: 0.7x, p < 0.05 F: 0.9x, p = 0.33	M: 0.7x, p < 0.05 F: 0.7x, p < 0.05	M: 0.9x, p < 0.05 F: 0.8x, p < 0.05	M: 0.4x, p < 0.05 F: 0.7x, p =0.16	M: 0.4x, p < 0.01 F: 0.5x, p < 0.05
iNOS	ING WAT	M: 0.7x, p < 0.01 F: 0.9x, p = 0.35	M: 0.5x, p < 0.01 F: 0.5x, p < 0.01	M: 0.7x, p < 0.01 F: 0.6x, p < 0.01	M: 0.7x, p < 0.01 F: 0.9x, p = 0.25	M: 0.6x, p < 0.01 F: 0.7x, p < 0.01
iNOS	PG WAT	M: 0.7x, p < 0.01 F: 0.8x, p < 0.01	M: 0.8x, p < 0.05 F: 0.8x, p < 0.05	M: 0.7x, p < 0.01 F: 0.6x, p < 0.01	M: 0.6x, p < 0.01 F: 0.7x, p < 0.01	M: 0.5x, p < 0.01 F: 0.6x, p < 0.01
FNDC5	Muscle	M: 1.4x, p < 0.05 F: 1.1x, p = 0.21	M: 1.3x, p < 0.05 F: 1.3x, p < 0.05	M: 1.4x, p < 0.05 F: 1.4x, p < 0.05	M: 1.3x, p < 0.01 F: 1.1x, p =0.46	M: 1.2x, p < 0.05 F: 1.2x, p < 0.05
FNDC5	Cerebral Cortex	M: 1.3x, p < 0.05 F: 1.1x, p = 0.24	M: 1.3x, p < 0.05 F: 1.4x, p < 0.01	M: 1.7x, p < 0.01 F: 1.7x, p < 0.01	M: 1.4x, p < 0.05 F: 1.1x, p =0.19	M: 1.2x, p < 0.05 F: 1.3x, p < 0.05
BDNF	Cerebral Cortex	M: 1.4x, p < 0.01 F: 1.1x, p = 0.51	M: 1.4x, p < 0.05 F: 1.3x, p < 0.05	M: 1.4x, p < 0.05 F: 1.4x, p < 0.05	M: 1.5x, p < 0.05 F: 1.0x, p =0.81	M: 1.4x, p < 0.05 F: 1.5x, p < 0.05
DCX	Cerebral Cortex	M: 1.3x, p < 0.05 F: 1.1x, p =0.15	M: 1.3x, p < 0.05 F: 1.3x, p < 0.05	M: 1.3x, p < 0.05 F: 1.4x, p < 0.05	M: 1.3x, p < 0.05 F: 1.1x, p =0.50	M: 1.4x, p < 0.05 F: 1.3x, p < 0.01

A



B

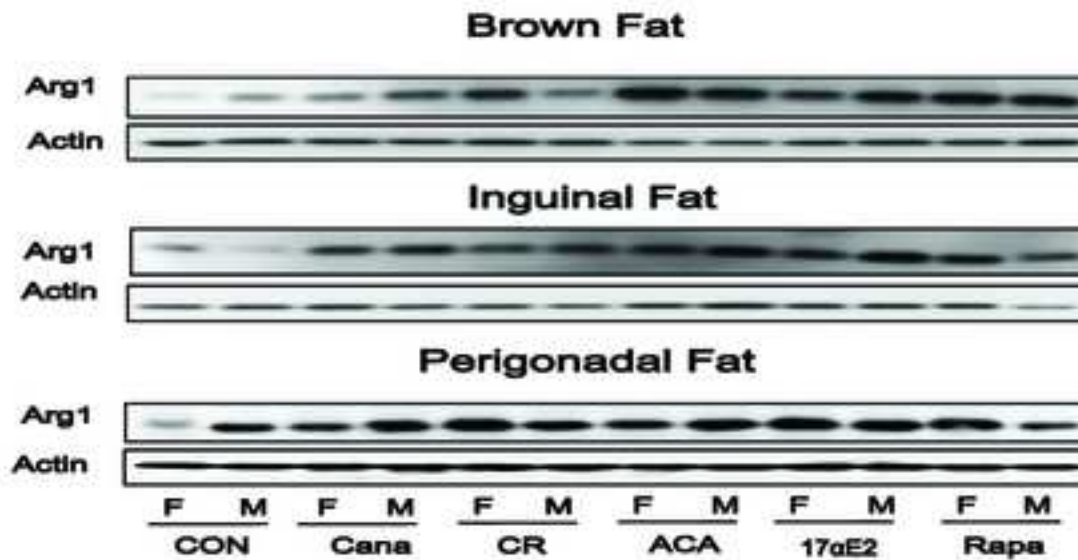


Drug	Interaction (Brown fat)	Sex (Brown fat)	Drug (Brown fat)
Cans	$p=0.05$	$p=0.02$	$p<0.05$
CR	$p=0.01$	$p=0.05$	$p<0.05$
ACA	$p=0.05$	$p=0.52$	$p<0.05$
17dE2	$p=0.01$	$p=0.17$	$p<0.01$
Rapa	$p=0.17$	$p=0.70$	$p<0.01$

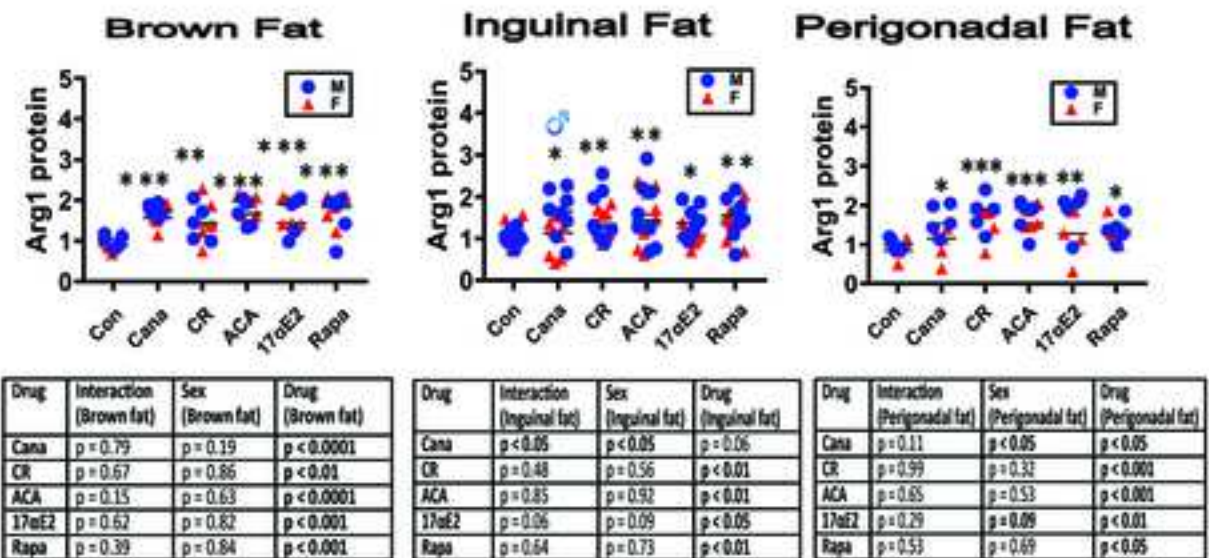
Drug	Interaction (Inguinal fat)	Sex (Inguinal fat)	Drug (Inguinal fat)
Cans	$p<0.001$	$p=0.09$	$p<0.01$
CR	$p<0.001$	$p=0.11$	$p<0.001$
ACA	$p=0.01$	$p=0.11$	$p<0.001$
17dE2	$p<0.001$	$p=0.11$	$p<0.001$
Rapa	$p=0.15$	$p=0.11$	$p<0.001$

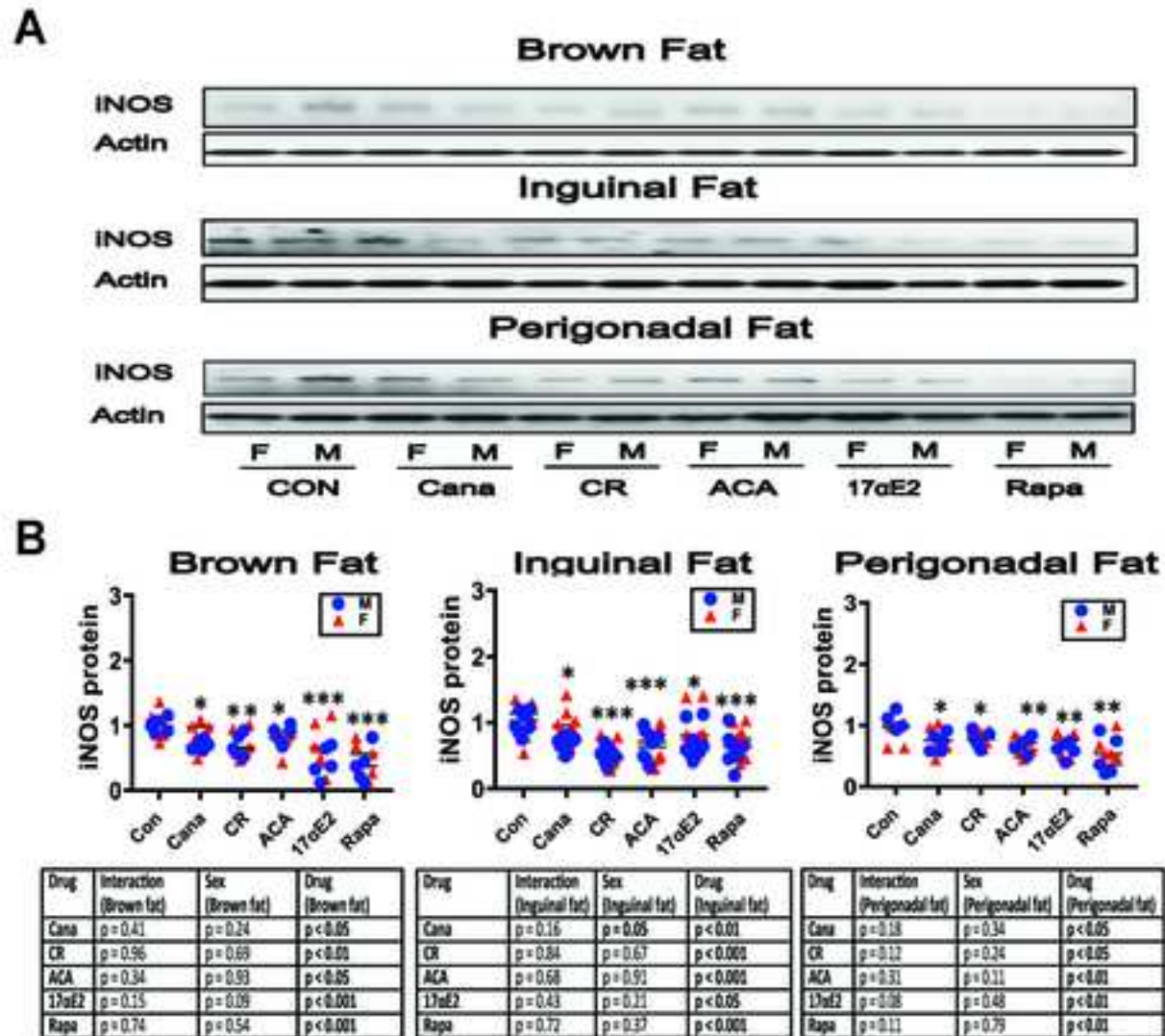
Drug	Interaction (Perigonadal fat)	Sex (Perigonadal fat)	Drug (Perigonadal fat)
Cans	$p<0.01$	$p<0.001$	$p<0.01$
CR	$p<0.01$	$p<0.01$	$p<0.01$
ACA	$p<0.11$	$p=0.02$	$p<0.05$
17dE2	$p<0.01$	$p<0.01$	NS
Rapa	$p<0.04$	$p=0.72$	$p<0.001$

A



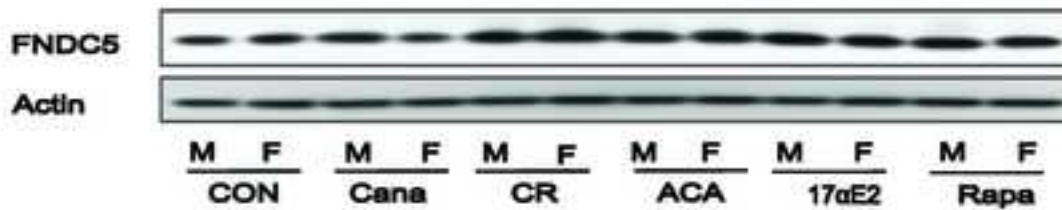
B



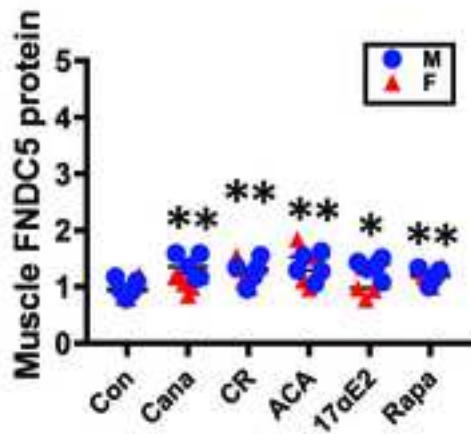


A

Muscle

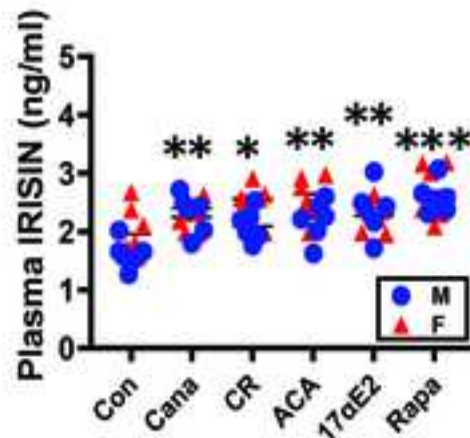


B

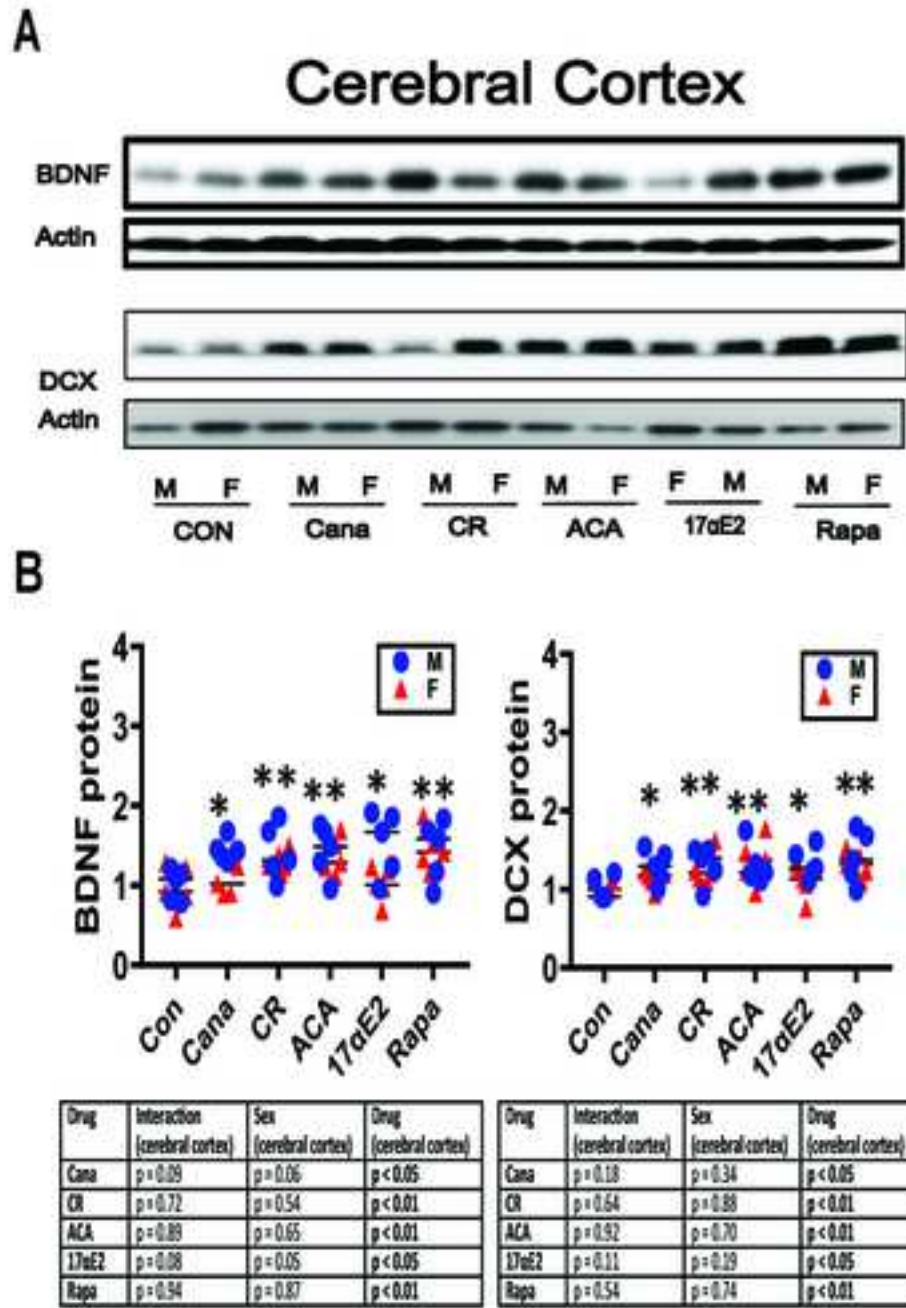


Drug	Interaction (muscle)	Sex (muscle)	Drug (muscle)
Cana	p = 0.14	p = 0.06	p < 0.01
CR	p = 0.88	p = 0.79	p < 0.01
ACA	p = 0.72	p = 0.99	p < 0.01
17αE2	p = 0.13	p = 0.06	p < 0.05
Rapa	p = 0.88	p = 0.70	p < 0.01

C

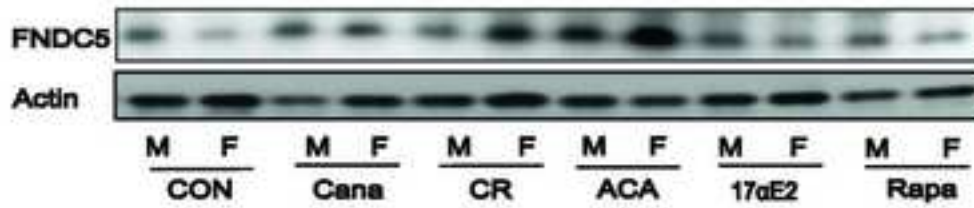


Drug	Interaction (Plasma)	Sex (Plasma)	Drug (Plasma)
Cana	p = 0.07	p = 0.19	p < 0.01
CR	p = 0.41	p = 0.06	p < 0.05
ACA	p = 0.58	p = 0.06	p < 0.01
17αE2	p = 0.06	p = 0.31	p < 0.01
Rapa	p = 0.29	p = 0.09	p < 0.001

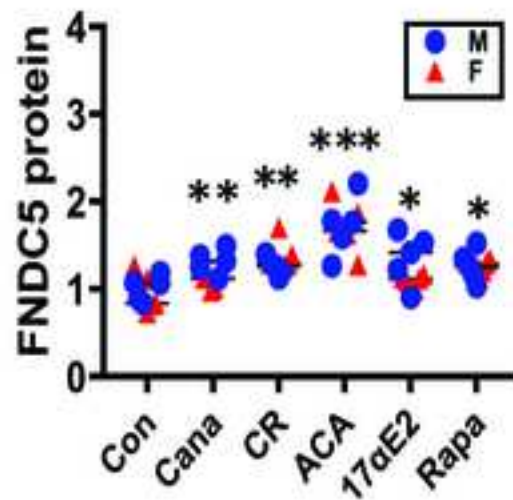


A

Cerebral Cortex



B



Drug	Interaction (cerebral cortex)	Sex (cerebral cortex)	Drug (cerebral cortex)
Cana	$p = 0.28$	$p = 0.06$	$p < 0.01$
CR	$p = 0.21$	$p = 0.61$	$p < 0.01$
ACA	$p = 0.84$	$p = 0.78$	$p < 0.001$
17αE2	$p = 0.31$	$p = 0.11$	$p < 0.05$
Rapa	$p = 0.73$	$p = 0.67$	$p < 0.01$